Springer

KSME

Journal of Mechanical Science and Technology 27 (8) (2013) 2391~2399
www.springerlink.com/content/1738-494x
DOI 10.1007/s12206-013-0624-7

Workspace quality analysis and application for a completely restrained 3-Dof planar cable-driven parallel manipulator †

Xiaoqiang Tang[1,*], Lewei Tang[1], Jinsong Wang[1] and Dengfeng Sun[2]

[1]*The State Key Laboratory of Tribology, Department of Mechanical Engineering, Tsinghua University, Beijing, 100084, China*
[2]*School of Aeronautics and Astronautics Engineering, Purdue University, West Lafayette, IN 47907-2045, USA*

(Manuscript Received August 13, 2012; Revised February 24, 2013; Accepted March 29, 2013)

Abstract

With the advantage of large workspace, low energy consumption and small inertia, the cable-driven parallel manipulator (CDPM) is suitable for heavy workpieces in rapid velocity and acceleration. We present a workspace analysis approach to solve force and torque equilibriums of completely restrained CDPMs. By this approach, not only the distribution but also the value of tensions driven by cables is investigated together. Two new indices, all cable tension distribution index (ACTDI) and area of the global quality workspace (AG) are proposed to evaluate the quality of the workspace. By concentrating on the workspace and its quality combined with the tension characteristics, these criteria are used to determine the optimal workspace in CDPMs. To verify the capacity of the proposed method, simulation examples are presented and the results demonstrate the approach's effectiveness. In the end, the dimensional design for a planar CDPM is discussed with the indices of workspace quality.

Keywords: Cable-driven parallel manipulator; Parallel manipulator; Workspace quality; Dimensional design

1. Introduction

It is well known that the rigid parallel mechanism has its own features, that is, high stiffness and heavy loading, while its workspace is relatively small in comparison with serial counterparts [1]. If the rigid linkages are substituted by flexible cables to control the pose of the moving platform, the flexible cables will make parallel manipulators realize a large workspace since the length of cables can be long. Compared with rigid-link parallel manipulators, cable-driven parallel manipulators (CDPMs) reveal some promising advantages in practical applications, such as in industry [2], astronomical observation [3-5] and pose measurement [6]. Such advantages are as follows: (1) Instead of heavy linkages, cables with light weights can accomplish green industry manufacturing in low energy consumption but high velocity/acceleration; (2) Larger workspace can be achieved by CDPMs mostly constrained only by cable length and tension limitation. Recently, CDPMs have been investigated in many aspects including workspace [7-10], tension optimization [11], control strategy [12] and so on. Moreover, it has been shown that m cables can control m-1 DOFs (completely restrained CDPMs) or less than m-1 DOFs (redundant restrained CDPMs) [13, 22, 23]. As shown in Fig. 1, one kind of completely restrained CDPMs is investigated in this paper, namely planar 4-3-CDPMs, where the planar 4-3-CDPM driven by four cables can maintain three DOFs (2 translation DOFs and one rotation DOF).

Compared with rigid-link parallel manipulators, CDPMs workspace should consider cable tension distribution situations. In other words, different tension distribution situation will get different workspace of CDPMs.

Based on the current research about CDPMs workspaces, the key issue is how to solve the wrench-close condition with positive tensions. Pham uses the maximum and the minimum tension index to discuss 4-3-CDPPM workspace with the null space method and proposes a recursive dimension reduction algorithm with Gaussian elimination to study the force-close workspace [14, 15]. Bosscher proposes the available net wrench set to calculate the wrench-feasible workspace [16]. Recently, Lau investigated a new hybrid analytical-numerical approach to define the workspace [17]. These approaches have proven to be valid for the workspace problem. However, the workspace is defined by the null space method only using point-wise evaluation techniques, and it is less effective and the accuracy for this method is based on the searching step-size. Moreover, the indices only use the maximum and the minimum tensions and ignore other tensions. Furthermore, the stiffness is another important issue for evaluating workspace quality of CDPMs, which has a major effect on the stability of

*Corresponding author. Tel.: +86 010 62792678, Fax.: +82 010 62792678
E-mail address: tang-xq@mail.tsinghua.edu.cn
† Recommended by Associate Editor Ki-Hoon Shin

CDPMs [18, 19]. Recent research shows that a rigid parallel mechanism can be optimized from its dexterity and stiffness to determine geometric parameters [20]. However, the method aforementioned is difficult to apply in CDPMs. Thus, it will be more effective and valuable if we can discuss the workspace quality considering both the tension distribution and the stiffness at the same time.

In this paper, the tension conditions based on force and torque equilibrium and the kinematics model are discussed in section 2. By tension analysis, the all cable tension distribution index (ACTDI) representing tension distribution and workspace quality analysis based on ACTDI is proposed in section 3. Combined with the stiffness index (SI), the area of global quality workspace (AG) is defined and analyzed in Section 4. By using the indices aforementioned, the dimensional optimal design is discussed in section 5. Finally, the conclusions are drawn in section 6.

2. Tension condition

2.1 Kinematical modeling

As illustrated in Fig. 1, a typical planar completely restrained cable-driven parallel manipulator consists of a fixed platform and a moving platform connected by several cables, where the cables control the DOFs of the moving platform by tensions and lengths.

The kinematics model of CDPM is shown in Fig. 2. The origin of the global frame {*G*} *O-XYZ* is placed at B_1, while the origin of the local frame {*P*} *O'-X'Y'Z'* is attached to the geometric center of the moving platform. $\boldsymbol{a}_i$ is a vector from the origin *O* to base platform joints B_i. ${}^{O'}\boldsymbol{r}_i$ is a vector from the origin *O'* to moving platform joints A_i, and $\boldsymbol{p}$ is a translation vector between the origins of two Cartesian coordinates.

The directional unit vector $\boldsymbol{u}_i$ along the cable *i* can be expressed as the following equation:

$$\mathbf{u}_i = \frac{\mathbf{a}_i - \mathbf{p} - {}^{G}\mathbf{R}_P\,{}^{P}\mathbf{r}_i}{\left\|\mathbf{a}_i - \mathbf{p} - {}^{G}\mathbf{R}_P\,{}^{P}\mathbf{r}_i\right\|} \quad (i = 1,2,3,4) \tag{1}$$

$${}^{G}\mathbf{R}_P = \begin{bmatrix} \cos\phi & -\sin\phi \\ \sin\phi & \cos\phi \end{bmatrix} \tag{2}$$

where ${}^{G}\boldsymbol{R}_P$ is a rotation matrix and ϕ is the orientation angle of moving platform.

2.2 Force and torque equilibrium

In Fig. 3, given an external wrench ($\boldsymbol{f}$, $\boldsymbol{m}$)' acting on the moving platform, *m* cable tensions can control *n* DOFs of a CDPM, which must satisfy the force and torque equilibrium below

$$\begin{aligned} &\sum_{i=1}^{m} \mathbf{t}_i + \mathbf{f} = \mathbf{0} \\ &\sum_{i=1}^{m} \mathbf{r}_i \times \mathbf{t}_i + \mathbf{m} = \mathbf{0}\,. \end{aligned} \tag{3}$$

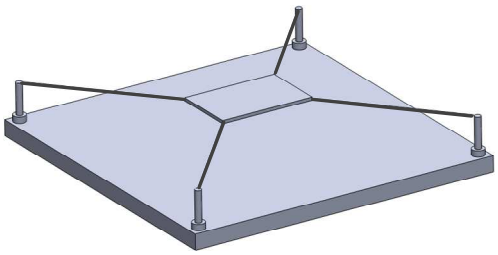

Fig. 1. Planar completely restrained 4-3-CDPMs.

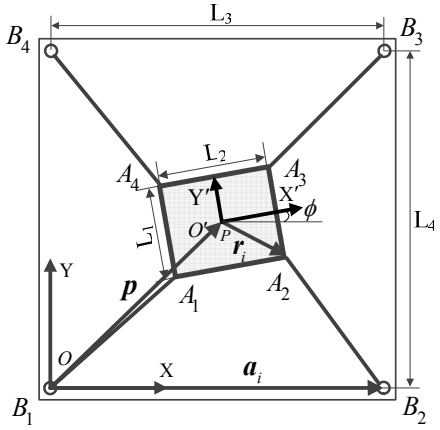

Fig. 2. Kinematic model of 4-3-CDPM.

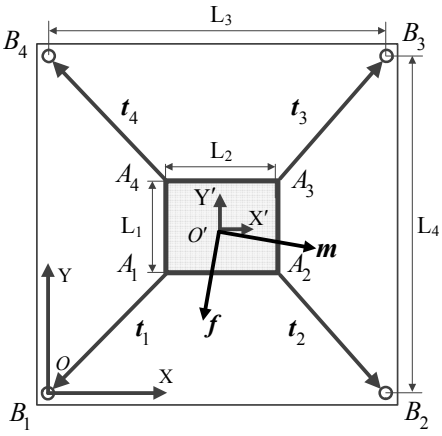

Fig. 3. Static model of the 3-Dof CDPM.

Substituting $\boldsymbol{t_i} = t_i\,\boldsymbol{u}_i$ into Eq. (3) leads to

$$\begin{bmatrix} \mathbf{u}_1 & \cdots & \mathbf{u}_m \\ \mathbf{r}_1 \times \mathbf{u}_1 & \cdots & \mathbf{r}_m \times \mathbf{u}_m \end{bmatrix} \begin{bmatrix} t_1 \\ \vdots \\ t_m \end{bmatrix} = -\begin{bmatrix} \mathbf{f} \\ \mathbf{m} \end{bmatrix}. \tag{4}$$

2.3 The approach for calculating cable tensions

When cable tensions satisfy Eq. (4) and sustain positive values, the pose must be part of the workspace with the orientation. Generally, it is difficult to solve Eq. (4) to obtain the workspace and tensions together. We used a concise approach

to solve this problem.

As for the CDPMs with complete constraints, m cables can control m-1 DOFs of the moving platform. Hence, Eq. (4) can be presented as a simple form Eq. (5) regardless of the external wrench

$$\begin{bmatrix} a_{11} & \cdots & a_{1m} \\ \vdots & \ddots & \vdots \\ a_{(m-1)1} & \cdots & a_{(m-1)m} \end{bmatrix} \begin{bmatrix} t_1 \\ \vdots \\ t_m \end{bmatrix} = \mathbf{0} \tag{5}$$

where $\begin{bmatrix} a_{11} & \cdots & a_{1m} \\ \vdots & \ddots & \vdots \\ a_{(m-1)1} & \cdots & a_{(m-1)m} \end{bmatrix} = \begin{bmatrix} \mathbf{u}_1 & \cdots & \mathbf{u}_m \\ \mathbf{r}_1 \times \mathbf{u}_1 & \cdots & \mathbf{r}_m \times \mathbf{u}_m \end{bmatrix}$

By moving the m column of the first matrix to the right side of the equation, Eq. (6) is taken as

$$\begin{bmatrix} a_{11} & \cdots & a_{1(m-1)} \\ \vdots & \ddots & \vdots \\ a_{(m-1)1} & \cdots & a_{(m-1)(m-1)} \end{bmatrix} \begin{bmatrix} t_1 \\ \vdots \\ t_{(m-1)} \end{bmatrix} = -t_m \begin{bmatrix} a_{1m} \\ \vdots \\ a_{(m-1)m} \end{bmatrix}. \tag{6}$$

Eq. (6) reveals that if some cable tension is determined in some pose, other tensions can be calculated only if the matrix is not singular. When all cable tensions are positive, the position and orientation are included in the workspace.

To prevent cable looseness, the minimum tension $t_{\min}$ should be assured in trajectory tracking. Meanwhile, the maximum tension $t_{\max}$ is also determined to avoid cable breakage. Thus, the tension range is retained as a constraint

$$0<t_{\min}\le t_i\le t_{\max}\ (i=1,2,\ldots,m). \tag{7}$$

Taking Eqs. (5)-(7) into consideration, the workspace and the tensions on arbitrary points are obtained, and the calculation steps are as follows:

Step 1: If t_{m} is the tension with the smallest value among all tensions, t_{m} is assigned as $t_{\min}$ and other tensions are calculated from Eq. (6);

Step 2: If the results have some negative values, the points are not in the workspace, and then the next point is tested;

Step 3: If the results are all positive, the points are included in the workspace, and then step 4 follows;

Step 4: If the results are all positive but some tension $t_i (i \neq m)$ is less than $t_{\min}$, remove the i column to the right side of Eq. (5) and restart step 1.

Sufficiency:

If some cable with the smallest tension is assigned as $t_{\min}$, other tensions are obtained in the calculation with unique magnitude so that the workspace is defined.

Necessity:

If the smallest tension of a cable is larger than $t_{\min}$, namely $t'_{\min} > t_{\min}$, then other tensions can be obtained with a single result as well. However, the result with $t'_{\min}$ is proportional to the result with $t_{\min}$, and the workspace is the same as before. Moreover, each tension from $t'_{\min}$ is larger than the respective tension from $t_{\min}$. From the point of practical usage like energy consumption, the result with $t_{\min}$ is better than the others.

Table 1. Comparison of ACTDI and TF.

Pose			Tension (N)				TF	ACTDI
x(m)	y(m)	ϕ	t_1	t_2	t_3	t_4		
0.579	0.380	1°	2.15	2.25	2.17	1	0.449	0.597
0.439	0.304		2.23	1.78	1.18	1	0.449	0.564

3. Workspace quality index of all cable tension distribution index (ACTDI)

3.1 All cable tension distribution index (ACTDI)

When the workspace of CDPMs in some configurations is determined, we encounter another problem, which is how to measure the workspace quality. Verhoeven introduces three indices to compare the quality of different CDPMs: the ratio index (RI), the quality index (QI), and the global quality index (GQI) [18]. Additionally, the ratio index r_{ws} shows that the tension limitation affects the workspace range.

Pham proposes tension factor (TF) and global tension index (GTI) to determine the workspace quality [8]. Tension factor, to the extent, reflects tension distribution by the minimum tension over the maximum tension. To further study the distribution of all cable tensions and analyze the effect of the distribution, the all cable tension distribution index (ACTDI) e_t is defined as the variance of all tensions over the minimum tension.

$$e_t = \frac{\sqrt{\sum_{i=1}^{m}(t_i-\bar{t})^2/(m-1)}}{\min(t_i)} \quad (i=1,2,\ldots,m) \tag{8}$$

where $\bar{t}$ is the average value of tensions. If e_t is smaller, the tensions are closer to each other.

For instance, when the moving platform is at the pose of (x = 0.579, y = 0.380) and (x = 0.439, y = 0.304) with $\phi = 1^\circ$, the tensions at two poses are listed in Table 1. Although TF is the same at these two poses, ACTDI implies that the latter pose has a better tension balance leading to a better control character. In light of this, we confirm that ACTDI is more feasible for defining the tension distribution for CDPMs.

3.2 Workspace quality analysis based on ACTDI

From the definition of ACTDI, tension distribution is more uniform when the index value is smaller. Given the dimensional parameter on Table 2, ACTDI over the workspace is calculated and shown in Fig. 4.

In Fig. 4, the value of ACTDI increases over the points from inside to outside. Furthermore, this index denotes that

Table 2. Dimensional parameter value.

L_1	L_2	L_3	L_4	ϕ
0.3 (m)	0.4 (m)	1 (m)	1 (m)	0°

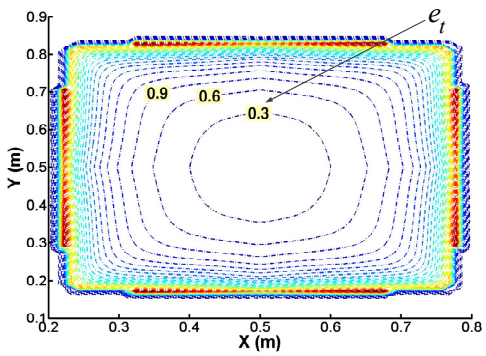

Fig. 4. Workspace with ACTDI as $\phi = 0^\circ$.

the points inside have smaller value and uniform tension distribution.

4. Workspace quality index of the area of global quality workspace (AG)

4.1 Stiffness index

To obtain a good tension distribution and maintain the stability, the global quality workspace is proposed by considering both the ACTDI and SI quality workspaces.

CDPMs are more flexible than other parallel manipulators. In light of this, the stiffness of CDPMs becomes an important issue in design and workspace quality analysis. Different from global flexibility indices in stiffness model of rigid parallel manipulators [21], the stiffness index (SI) S_t is proposed to depict stiffness in CDPMs. According to Verhoeven [18], the stiffness matrix is denoted as

$$\boldsymbol{K} = k'\boldsymbol{A}^{\mathrm{T}}\boldsymbol{L}^{-1}\boldsymbol{A}, \tag{9}$$

where k' is the stiffness of a cable with one unit length.

$$\mathbf{A}^{\mathrm{T}} = \begin{bmatrix} \mathbf{u}_1 & \dots \mathbf{u}_m \\ \mathbf{r}_1 \times \mathbf{u}_1 & \dots \mathbf{r}_m \times \mathbf{u}_m \end{bmatrix}$$

$$\mathbf{L}^{-1} = \begin{bmatrix} l_1^{-1} & \dots & 0 \\ \vdots & \ddots & \vdots \\ 0 & \dots & l_m^{-1} \end{bmatrix}$$

where $l_1, \dots, l_m$ refers to the lengths of $1^{th}, \dots, m^{th}$ cable.

Then, the eigenvalues of stiffness matrix are obtained as $0 \le k_{e1} \le \dots \le k_{en}$. The stiffness index S_t is defined as the evolution of the minimum eigenvalue over the maximum eigenvalue.

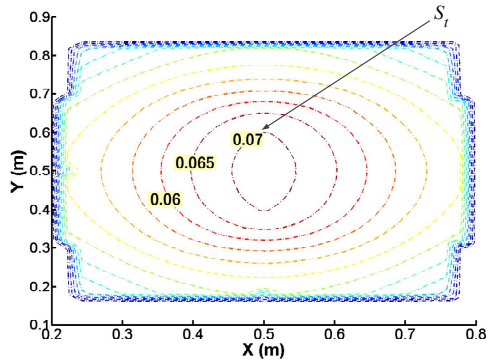

Fig. 5. Workspace with SI as $\phi = 0^\circ$.

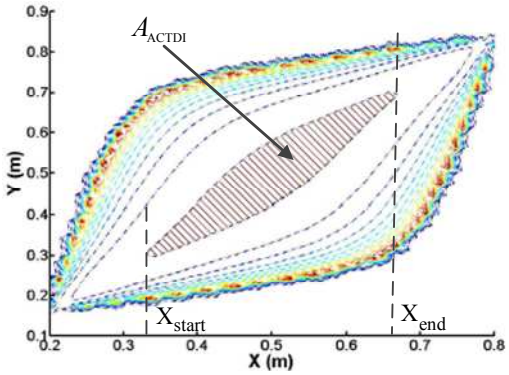

Fig. 6. ACTDI quality workspace.

$$S_t = \sqrt{\frac{\min(k_{ei})}{\max(k_{ei})}} \quad (i=1,2,\dots,n). \tag{10}$$

4.2 Workspace quality analysis based on SI

The stiffness index (SI) reflects the ability to resist external wrench for points in the workspace. The range of the stiffness index is limited between 0 and 1. When it is close to 1, it means that the stiffness of the point is more isotropic. In other words, an external wrench applied on the moving platform has the same effect on the end-effector in all directions. The stiffness index distribution over the workspace is shown in Fig. 5, and the dimensional parameter is the same as in Table 1.

From the discussion above on Figs. 4 and 5, the conclusion is drawn that ACTDI and SI change in different directions over the workspace. Nevertheless, in practical applications, tensions and the stiffness in all directions are usually more feasible to be uniform. Hence, integrated with these two indices, a compromise is necessary for an optimal workspace.

4.3 The area of global quality workspace (AG)

As for quality workspace aforementioned, the area of ACTDI quality workspace is surrounded by ACTDI curve with the same value of ACTDI in Fig. 6. So, A_{ACTDI} is the integral of the area with ACTDI equal to or less than the required, where the distribution of tensions is revealed.

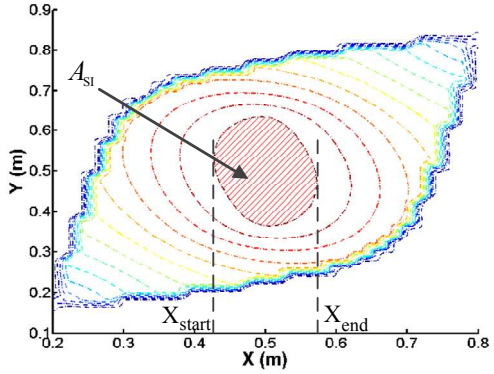

Fig. 7. SI quality workspace.

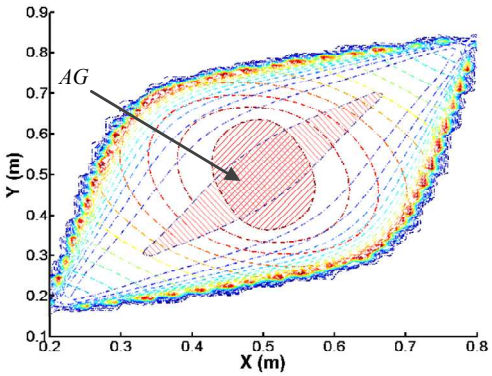

Fig. 8. AG quality workspace.

$$A_{ACTDI} = \int_{X_{start}}^{X_{end}} y d(X) \tag{11}$$

Similar to A_{ACTDI}, the area of SI quality workspace is surrounded by the SI curve in Fig. 7. A_{SI} is the integral of the area with SI equal to or greater than the required value, where the stiffness of this CDPM is shown.

$$A_{si} = \int_{X_{start}}^{X_{end}} y d(X) . \tag{12}$$

The area of the global quality workspace (AG) is proposed by considering both the area of ACTDI and SI quality workspaces as shown in Fig. 8.

$$AG = A_{ACTDI} \cap A_{SI} . \tag{13}$$

5. Dimensional design application for optimal AG

From the simulation example above, the workspace quality is investigated with these indices for optimal dimension design. In this section, the length and the width of both the moving platform and the fixed platform are changed. μ_1 is defined by the length over the width of the moving platform, μ_2 by the width of the moving platform over the length of the fixed platform and μ_3 by the width over the length of the fixed platform, that is

Table 3. A_{ACTDI} with μ_1.

A_{ACTDI} (mm^2)		μ_1		
		1.33	2	2.5
ϕ	0°	86024	60904	41935
	1°	74771	59779	41691
	2°	34657	56295	40509
	4°	0	41259	35959
	6°	0	11588	28317

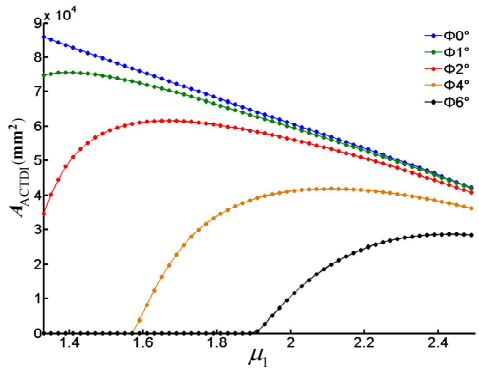

Fig. 9. A_{ACTDI} with various μ_1.

$$\mu_1 = L_2 / L_1 \tag{14a}$$

$$\mu_2 = L_1 / L_3 \tag{14b}$$

$$\mu_3 = L_4 / L_3 . \tag{14c}$$

From the workspace quality analysis, two crucial indices, ACTDI and SI, are selected as the most important parameters to define quality workspace. Thus, the trend about ACTDI and the maximum SI with μ_1, μ_2 and μ_3 are studied in this section firstly.

Furthermore, two quality workspaces are denoted as A_{ACTDI} and A_{SI}. The former one is defined as the area that the ACTDI is equal to or less than 0.5, and the latter one as the area that the SI is equal to or more than 0.2 (estimation standards ACTDI and SI can be varied according to practical requirements). In the end, these two quality workspaces are investigated together to determine the optimal workspace that both ACTDI and SI are satisfied respectively, where it is called AG.

5.1 Ratio μ_1

In this section we take advantage of these indices to measure the workspace quality about a planar CDPM. As shown in Fig. 1, the 4-3-CDPM has four cables with three DOFs, including two translation DOFs and one rotation DOF. The kinematical model about this CDPM is illustrated in Fig. 2.

Given the minimum tension t_{min} = 1N and the maximum allowed tension t_{max} = 20N, A_{ACTDI} is obtained based on the approach mentioned above from Matlab in Table 3 and μ_1

Table 4. A_{SI} with μ_1.

A_{SI} (mm^2)		μ_1		
		1.33	2	2.5
ϕ	0°	0	31911	117028
	1°	0	32031	116231
	2°	0	32523	114315
	4°	0	34707	107957
	6°	0	40691	96123

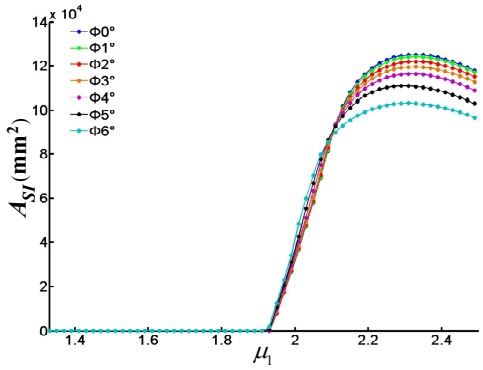

Fig. 10. A_{SI} with various μ_1.

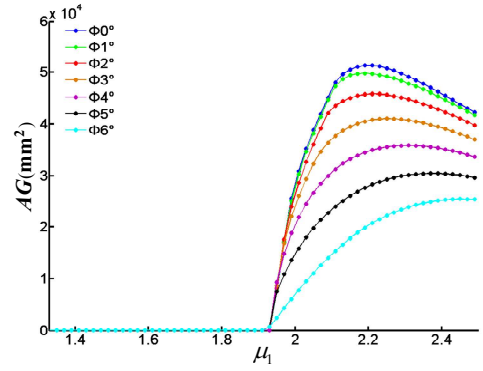

Fig. 11. AG with various μ_1.

varies from 2.5 to 1.33 with a decrement of 0.02 in Fig. 9.

Different from A_{ACTDI}, A_{SI} shows that the area has a more uniform stiffness over the workspace. The SI quality workspace is obtained in Table 4 and Fig. 10. When the ratio μ_1 is valued between 2.2 and 2.3, the SI quality workspace achieves the maximum value at different angles.

As shown in Fig. 11, AG obtains the maximum value as μ_1 between 2.1 and 2.3. Moreover, AG comes to monotonously increasing as an orientation angle larger than 6° .

5.2 Ratio μ_2

Suppose the width of the moving platform is fixed as 0.3 m and the length as 0.4 m, the workspace with the ACTDI is discussed concerning different μ_2 from 0.3 to 0.15 with a decrement of 0.005. To compare in detail, μ_2 is selected with some values as in Table 5.

Table 5. Selected μ_2.

μ_2	0.3	0.25	0.2	0.15
L1 (m)	0.3			
L3 (m)	1	1.2	1.5	2

Table 6. A_{ACTDI} with μ_2.

A_{ACTDI} (m^2)		μ_2			
		0.3	0.25	0.2	0.15
ϕ	1°	0.0748	0.1283	0.2332	0.4811
	2°	0.0357	0.0607	0.1095	0.2223
	4°	0	0	0	0

Table 7. Maximum S_t with μ_2.

Maximum S_t		μ_2			
		0.3	0.25	0.2	0.15
ϕ	0°	0.0714	0.0667	0.0625	0.0588
	2°	0.0733	0.0684	0.0642	0.0605
	4°	0.0785	0.0735	0.0690	0.0651

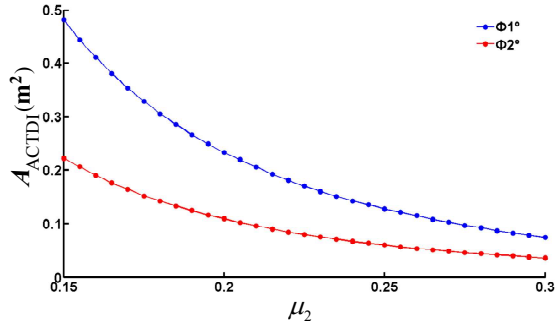

Fig. 12. A_{ACTDI} with various μ_2.

Then, the ACTDI quality workspace used before with different μ_2 is listed in Table 6. As shown in Fig. 12, the ACTDI quality workspace changes, in which the minimum e_t is larger than 0.5. In light of this, if this planar CDPM is applied in practice, a larger μ_2 suggests that the tension distribution is more uniform. Moreover, the tension distribution becomes worse with the angle increasing.

Since the stiffness index S_t over the workspace is less than 0.2 aforementioned, the maximum S_t with some μ_2 is listed in Table 7, while μ_2 varies from 0.3 to 0.15 with a decrement of 0.002 shown in Fig. 13. In addition, it reveals that a larger μ_2 can yield a larger maximum S_t. However, maximum stiffness in Fig. 13 implies that the SI quality workspace is always 0 because it is less than 0.2 of the definition above.

5.3 Ratio μ_3

Suppose the width and the length of the moving platform is fixed at 0.3 m and 0.4 m, respectively, and the length of the fixed platform is 1 m, the workspace with the ACTDI is discussed with different μ_3 from 1 to 1.4, and μ_3 is selected with

Table 8. Selected μ_3.

μ_3	1	1.2	1.4
L3 (m)	1		
L4 (m)	1	1.2	1.4

Table 9. A_{ACTDI} with μ_3.

A_{ACTDI} (m^2)		μ_3		
		1	1.2	1.4
ϕ	1°	0.0747	0.1088	0.1406
	2°	0.0357	0.0929	0.1309
	4°	0	0.0110	0.0814

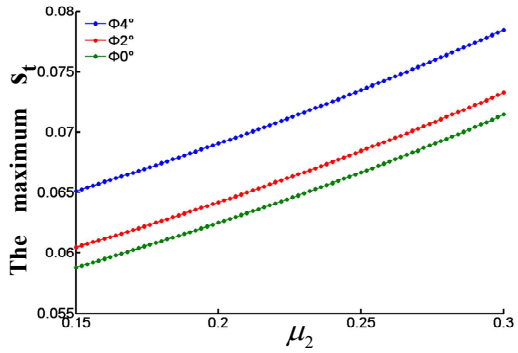

Fig. 13. Maximum S_t with various μ_2.

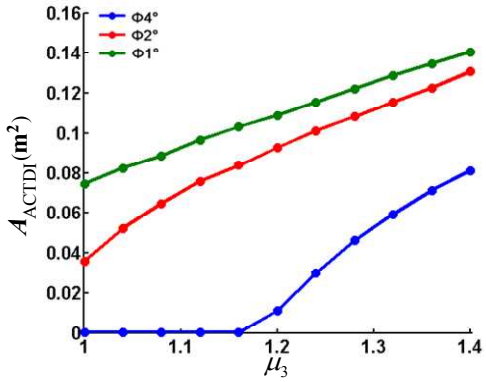

Fig. 14. A_{ACTDI} with various μ_3.

some values as in Table 8.

Then, the ACTDI quality workspace with different μ_3 is listed in Table 9. As shown in Fig. 14 with μ_3 from 1.4 to 1 with a decrement of 0.04, the ACTDI quality workspace increases with greater μ_3 and smaller orientation angle due to the larger area of the fixed platform.

Similar to μ_2, the stiffness index S_t over the workspace is less than 0.2, the maximum S_t in various μ_3 are listed in Table 10 and in Fig. 15, respectively. The results about μ_3 imply that the workspace quality is better with a greater area of the fixed platform for the same end-effector.

In summary, the global optimal dimensional design problem concerning this 3-Dof planar cable-driven manipulator is

Table 10. Maximum S_t with μ_3.

Maximum S_t		μ_3		
		1	1.2	1.4
ϕ	1°	0.0719	0.1002	0.1183
	2°	0.0733	0.1008	0.1186
	4°	0.0785	0.1030	0.1198

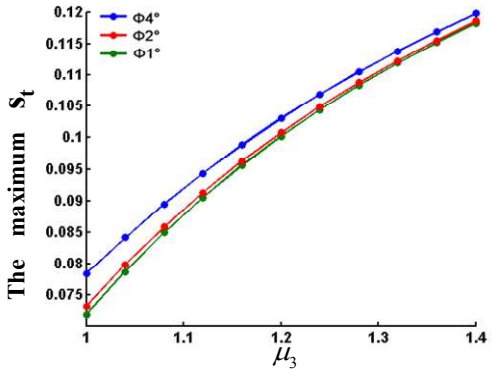

Fig. 15. Maximum S_t with various μ_3.

concluded to obtain the optimal L_1, L_2, L_3 and L_4. Thus, the optimization problem is transferred to find the best dimensional ratios-- μ_1, μ_2, μ_3--in parameter study. The discussion aforementioned about relative optimal parameters rests on the previous assumption that there exists a unique variant with other two ratios determined, which is similar to the process based on an exhaustive search in Ref. [24]. However, the optimal process turns out to be an intricate problem to attain a global optimal solution according to optimal AG. Recently, Lin [25, 26] proposed a genetic algorithm with differential evolution (GA-DE) hybrid algorithm to address this optimization problem with implicit objective function and constraints. This method will be employed to achieve global optimal parameters in the future research work.

6. Conclusions

According to the aforementioned workspace quality, we concentrate on using two new indices and apply the indices to optimize the dimensional design of a typical planar 4-3-CDPM. The conclusions can be drawn as follows:

(1) To measure the workspace quality, two new evaluation indices are proposed to depict the quality of the workspace, which are the all cable tension distribution index (ACTDI) and the area of global quality workspace (AG).

(2) Compared with previous research, AG is more feasible for CDPMs since both tension distribution and stiffness are taken into account as a whole. From the analysis of the simulation example above, the workspace quality with different orientations changes considerably in the representation of the indices. It has been revealed that it is more appropriate to determine an optimal workspace by considering the tension index and stiffness index altogether.

(3) The results demonstrate that the approach and the indices are not only easily used, but also can be applied in other completely restrained CDPMs. Also, the dimensional design procedure is presented for designing a relative optimal planar CDPM with high stiffness and more uniform tension distribution.

Future research will address the issue on the determination of the optimal workspace of spatial parallel mechanisms.

Acknowledgment

This work is supported by National Natural Science Foundation of China (No. 11178012, 50975149), and the National S&T Major Project of China (No. 2011ZX04015-011).

References

[1] Y. Hu, J. W. Zhan, Z. Wan and J. C. Lin, Design and analysis of a 6-DOF mobile parallel robot with 3 limbs, *Journal of Mechanical Science and Technology*, 25 (12) (2011) 3215-3222.

[2] T. Aria, H. Osumi and H. Yamaguchi, Assembly robot suspended by three wires with seven degrees of freedom, *Proceedings of the 11th international conference on assembly automation*, (1990) MS90-807.

[3] Q. J. Duan and X. C. Duan, Analysis of cable-actuated parallel robot with variable length and velocity cable, *Procedia Engineering*, 15 (2011) 2732- 2737.

[4] X. Q. Tang and R. Yao, Dimensional design on the six-cable driven parallel manipulator of FAST, *ASME Journal of Mechanical Design*, 133 (11) (2011) 1-12.

[5] X. Q. Tang, W. B. Zhu, C. H. Sun and R. Yao, Similarity model of feed support system for FAST, *Experimental Astronomy*, 29 (2011) 177-187.

[6] M. S. Varziri and L. Notash, Kinematic calibration of a wire-actuated parallel robot, *Mechanism and Machine Theory*, 42 (2007) 960-976.

[7] M. Gouttefarde and C. M. Gosselin, Analysis of the wrench-closure workspace of planar parallel cable-driven mechanisms, *IEEE Transactions on Robotics*, 22 (3) (2006) 434-445.

[8] C. B. Pham, S. H. Yeo, G. L. Yang and I-M. Chen, Workspace analysis of fully restrained cable-driven manipulators, *Robotics and Autonomous Systems*, 57 (2009) 901-912.

[9] W. B. Lim, G. L. Yang, S. H. Yeo and S. K. Mustafa, A generic force-closure analysis algorithm for cable-driven parallel manipulators, *Mechanism and Machine Theory*, 46 (2011) 1265-1275.

[10] J. Pusey, A. Fattah, S. Agrawal and E. Messina, Design and workspace analysis of a 6-6 cable-suspended parallel robot, *Mechanism and Machine Theory*, 39 (2004) 761-778.

[11] A. Alikhani, S. Behzadipour, A. Alasty and S. A. S. Vanini, Design of a large-scale cable-driven robot with translational motion, *Robotics and Computer-Integrated Manufacturing*, 27 (2011) 357-366.

[12] S. Lahouar, E. Ottaviano, S. Zeghoul, L. Romdhane and M. Ceccarelli, Collision free path-planning for cable-driven parallel robots, *Robotics and Autonomous Systems*, 57 (2009) 1083-1093.

[13] M. Hiller, S. Fang, S. Mielczarek, R. Verhoeven and D. Franitza, Design, analysis and realization of tendon-based parallel manipulators, *Mechanism and Machine Theory*, 40 (2005) 429-445.

[14] C. B. Pham, S. H. Yeo and G. L. Yang, Workspace analysis and optimal design of cable-driven planar parallel manipulator, *Proc. of the 2004 IEEE Inter. Conf. on Robotics, Automation, and Mechatronics*, (2004) 219-224.

[15] C. B. Pham, S. H. Yeo, G. L. Yang, M. S. Kurbanhusen and I-M. Chen, Force-closure workspace analysis of cable-driven parallel mechanisms, *Mechanism and Machine Theory*, 41 (2006) 53-69.

[16] P. Bosscher and I. Ebert-Uphoff, Wrench-based analysis of Cable-Driven Robots, *Proceedings of IEEE Conference on Robotics and Automation*, New Orleans, LA, (2004) 4950-4955.

[17] D. Lau and D. Oetomo, Wrench-closure workspace generation for cable driven parallel manipulators using a hybrid analytical-numerical approach, *Journal of Mechanical Design*, 133 (7) (2011) 071004/1-7.

[18] R. Verhoeven, *Analysis of the workspace of tendon-based Stewart platforms,* Ph.D. dissertation, Univ. Duisburg-Essen, Duisburg, Germany (2004).

[19] S. Behzadipour and A. Khajepour, Stiffness of cable-based parallel manipulators with application to stability analysis, *Journal of Mechanical Design*, 128 (2006) 303-310.

[20] J. H. Lee, Y. J. Nam and M. K. Park, Kinematics and optimization of a 2-DOF parallel manipulator with a passive constraining leg and linear actuators, *Journal of Mechanical Science and Technology*, 24 (1) (2010) 19-23.

[21] B. Li, H. J. Yu, Z. Q. Deng, X. J. Yang and H. Hu, Stiffness modeling of a family of 6-DoF parallel mechanisms with three limbs based on screw theory, *Journal of Mechanical Science and Technology*, 24 (1) (2010) 373-382.

[22] X. Q. Tang, L. W. Tang, J. S. Wang and D. F. Sun, Configuration synthesis for completely restrained cable-driven parallel manipulators with 7 cables, *International Journal of Advanced Robotic Systems*, 9 (142) (2012) 1-10.

[23] L. W. Tang, X. Q. Tang, J. S. Wang and X. M. Chai, Workspace analysis and tension optimization design in docking parallel mechanism driven by seven cables, *Chinese Journal of Mechanical Engineering*, 48 (21) (2012) 1-7.

[24] W. Y. Lin, C. L. Shen and K. M. Hsiao, A case study of the five-point double-toggle mould clamping mechanism, *Proc. of the Institute of Mechanical Engineers, Part C: Journal of Mechanical Engineering Science*, 220 (C4) (2006) 527-536.

[25] W. Y. Lin and S. S. Wang, Dimensional synthesis of the five-point double-toggle mould clamping mechanism using a genetic algorithm-differential evolution hybrid algorithm, *Proc. of the Institute of Mechanical Engineers, Part C: Journal of Mechanical Engineering Science*, 224 (6) (2010) 1305-1313.

[26] W. Y. Lin, A GA-DE hybrid evolutionary algorithm for path synthesis of four-bar linkage, *Mechanism and Machine Theory*, 45 (8) (2010) 1096-1107.

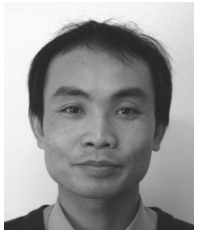

Xiaoqiang Tang received the B.S. and M.S. in Mechanical Engineering from Harbin University of Science and Technology, Harbin, China, in 1995 and 1998, respectively, and the Ph.D. in Mechanical Engineering from Tsinghua University, Beijing, in 2001. He is currently an Associate Professor in the Department of Mechanical Engineering, Institute of Manufacturing Engineering, Tsinghua University. His research interests include parallel manipulators, robots, and reconfigurable manufacturing technology.

Lewei Tang received the B.S. in Mechanical Engineering from Xi'an Jiaotong University, Xi'an, China, in 2010. He is currently working toward the Ph.D. in the Department of Mechanical Engineering, Institute of Manufacturing Engineering, Tsinghua University, Beijing. His research interests include parallel manipulators, cable-driven parallel manipulators, stiffness analysis and accuracy.